Symmetry-Guided *Ab Initio* Approach to Light and Medium-Mass Nuclei

T. Dytrych[a], J. P. Draayer[a], K. D. Launey[a] and D. Langr[b]

[a] *Department of Physics and Astronomy, Louisiana State University, Baton Rouge, LA 70803, USA*

[b] *Department of Computer Systems, Czech Technical University, Prague, Czech Republic*

Abstract

We use algorithms of computational group theory to perform *ab initio* no-core shell model calculations in a SU(3)-based coupling scheme for *p*-shell nuclei. Details given for ^{6}Li are reflective of similar results found for ^{8}B, ^{8}Be, ^{12}C, and ^{16}O, all of which exhibit a strong preference for large quadrupole deformations and a narrow set of intrinsic spin quantum numbers. Our results suggest that a small subspace of symmetry-adapted configurations can very closely approximate the exact solutions while allowing for exact factorization of the center-of-mass degrees of freedom. This, in turns, promises to allows us to extend the reach of the ab initio framework for structure and reaction studies towards *sd*-shell nuclei and beyond.

Keywords: *No-core shell model; SU(3) coupling scheme; p-shell nuclei*

1 Introduction

Theoretical advances achieved in recent years in the development of realistic nuclear potential models [1, 2, 3, 4] along with progress in high performance computing have placed *ab initio* many-particle approaches [5, 6, 7] at the frontier of nuclear structure explorations. The *ab initio* methods are built on fundamental principles and therefore hold promise to provide predictive capabilities essential for a description of the structure and reactions of unstable and exotic nuclei, many of which are of high interest, e. g., in nucleosynthesis, but remain inaccessible even to experiment.

The no-core shell model (NCSM) [5] is a prominent *ab initio* method that has achieved a good description of low-lying states and associated spectroscopic properties up through *p*-shell nuclei [8, 9, 10]. The NCSM typically employs the Lanczos algorithm to solve the eigenvalue problem for a realistic Hamiltonian. Matrix elements of the Hamiltonian are calculated in a many-particle basis of m-scheme states, which are constructed as an antisymmetrized product of the harmonic oscillator single-particle wave functions, and carry the z-component of the total angular momentum along with the total parity as good quantum numbers. The main limitation of this approach, and the predictive power thereof, is inherently coupled with the combinatorial growth in the size of the many-particle model space with increasing nucleon numbers and expansion in the number of single-particle levels in the model space.

We developed an innovative *ab initio* model, the symmetry-adapted no-core shell model (SA-NCSM), which utilizes a many-particle basis that exploits the physically relevant SU(3)$\supset$SO(3) group-subgroup chain. The significance of the SU(3) group for a microscopic description of the nuclear collective dynamics can be readily seen from the fact that it is the symmetry group of the Elliott model [11], and a subgroup of the Sp$(3,\mathbb{R})$ symplectic model of nuclear collective motion [12, 13]. The concept of symmetry-adapted many-particle basis represents a powerful tool that allows one to winnow a model space to correlations indispensable for modeling important modes of nuclear collective dynamics, specifically nuclear deformation and cluster substructures, thereby overcoming the scale explosion bottleneck of *ab initio* nuclear structure

computations. Hence, the SA-NCSM framework holds promise to expand dramatically the reach of current *ab initio* approaches toward describing heavier mass nuclei with unprecedented accuracy.

2 *Ab initio* calculations in SU(3)-scheme basis

The basis states of the SA-NCSM are constructed in the proton-neutron formalism and are labeled by the physical SU(3)⊃SO(3) subgroup chain quantum numbers $(\lambda\,\mu)\kappa L$, and by proton, neutron, and total intrinsic spins S_p, S_n, and S. The orbital angular momentum L is coupled with S to the total angular momentum J and its projection M_J. Each basis state is thus labeled in the SU(3)-scheme as

$$|\vec{\alpha}\, N(\lambda\,\mu)\kappa L; S_p S_n S; JM_J\rangle, \tag{1}$$

where N signifies the number of harmonic oscillator quanta with respect to the minimal number for a given nucleus. The deformation-related $(\lambda\,\mu)$ set of quantum numbers labels SU(3) irreducible representations (irreps) and bring forward important information about nuclear shapes and deformation. For example, (00), $(\lambda\,0)$ and $(0\,\mu)$ describe spherical, prolate and oblate shapes, respectively. The label κ distinguishes multiple occurrences of the same L value in the parent irrep $(\lambda\,\mu)$. The symbol $\vec{\alpha}$ schematically denotes the additional quantum numbers needed to unambiguously distinguish between irreps carrying the same $N\,(\lambda\,\mu)\,S_pS_nS$ quantum numbers. These irreps compose a well-defined subspace with a unique feature that allows for the complete separation of intrinsic and center-of-mass degrees of freedom [14].

The SA-NCSM implements a set of powerful algorithms [15, 16] which facilitate calculations of matrix elements of arbitrary (currently up to two-body, but expandable to higher-rank) operators in the SU(3)-scheme basis. This allows for both the evaluation of the Hamiltonian matrix elements, and the use of the resulting eigenvectors to evaluate other experimental observables. The underlying principle behind the SA-NCSM computational kernel is the SU(3) Wigner-Eckhart theorem, which allows the problem to be factorized into SU(3) reduced matrix elements (RMEs) and SU(3) coupling/recoupling coefficients. The former are calculated from a set of single-shell RMEs by the repetitive application of the SU(3) reduction formula for RMEs of operators acting on two independent proton and neutron subsystems, while the latter are computed using a publicly available library [17].

3 Structure of nuclear wave functions

Here we use the SA-NCSM with the bare JISP16 NN interaction [1] to calculate binding energies and determine low-lying eigenstates of ^{6}Li, ^{8}Be, ^{12}C, and ^{16}O nuclei. The resulting wave functions are used to determine values or physical observables such as point-particle root-mean-square (rms) matter radii, electric quadrupole moments, magnetic dipole moments, reduced electromagnetic $B(E2)$ and $B(M1)$ transition strengths.

The expansion of calculated wave functions in a physically relevant SU(3)-scheme basis is illuminating salient features that emerge from the complex dynamics of strongly interacting many-particle systems. To explore the nature of the most important correlations, the probability distribution of intrinsic spins $(S_p\,S_n\,S)$ and deformation-related $(\lambda\,\mu)$ quantum numbers of SU(3) for the lowest-lying $T = 0$ states of ^{6}Li were analyzed. Figure 1a shows the probability distribution of intrinsic spins across their Pauli-allowed deformations in the ground state of ^{6}Li. This figure illustrates a facet common to low-energy solutions considered: a highly structured and coherent mix of intrinsic spins and SU(3) spatial quantum numbers that has heretofore gone unrecognized in other *ab initio* studies. These results clearly corroborate

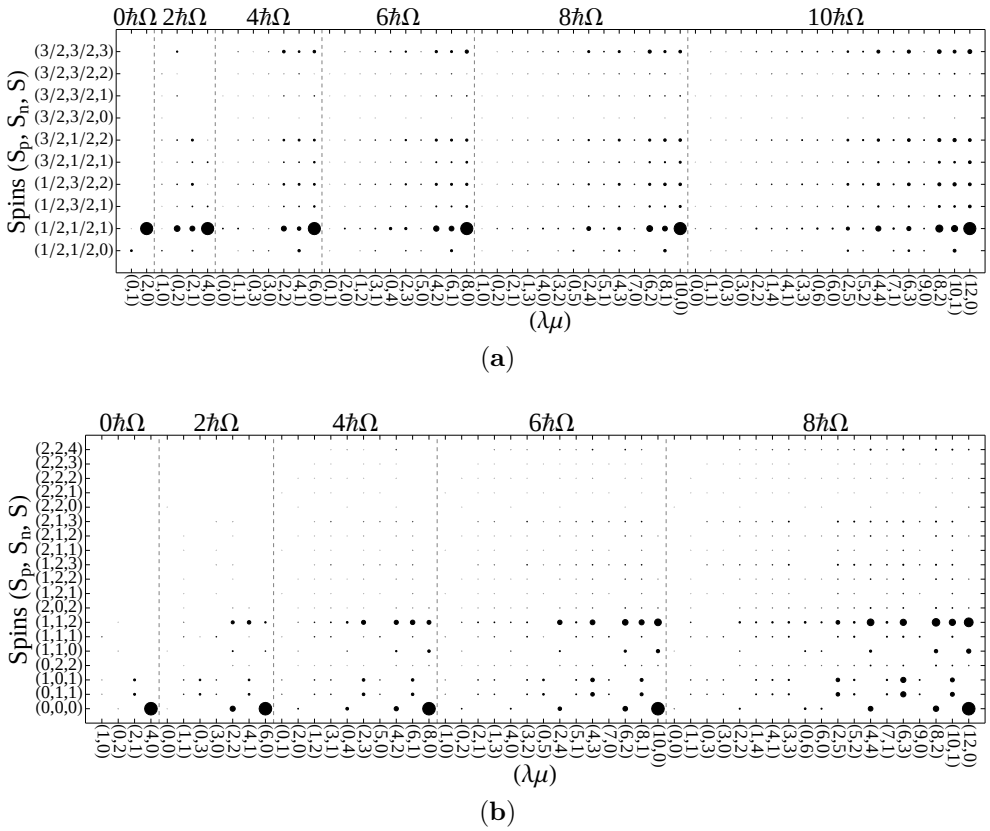

Figure 1: Probability distribution of proton, neutron, and total intrinsic spins $(S_p\, S_n\, S)$ across their Pauli-allowed $(\lambda\,\mu)$ deformations (horizontal axis) in the ground 1^+ state of ^{6}Li (a) and the ground 0^+ state of ^{8}Be (b) obtained with JISP16 bare interaction for $\hbar\Omega = 20$ MeV in $N_{\max} = 10$ (a) and $N_{\max} = 8$ (b) full model spaces. The area of each circle is proportional to the total probability of $N\,(\lambda\,\mu)\,S_pS_nS$ states normalized with respect to the total probability of $N\,(2+N\,0)\,\frac{1}{2}\,\frac{1}{2}\,1$ and $N\,(4+N\,0)\,0\,0\,0$ stretched states, respectively.

the much earlier phenomenological work carried out within the context of the Elliott SU(3) model [11].

Specifically, we found that over 99% of the SA-NCSM eigenstates are accounted for by a small fraction of intrinsic spin combinations. For instance, the lowest-lying eigenstates in ^{6}Li are almost entirely realized in terms of configurations characterized by the following intrinsic spin $(S_p\, S_n\, S)$ quantum numbers: $(\frac{3}{2}\,\frac{3}{2}\,3)$, $(\frac{1}{2}\,\frac{3}{2}\,2)$, $(\frac{3}{2}\,\frac{1}{2}\,2)$, and $(\frac{1}{2}\,\frac{1}{2}\,1)$, with the last one carrying over 90% of each eigenstate. Likewise, the same spin components as in the case of ^{6}Li are found to dominate the ground state and the lowest 1^+, 3^+, and 0^+ excited states of ^{8}B (Table 1). Similarly, the ground state band of ^{8}Be and ^{12}C along with the ground state of ^{16}O are found to be dominated by many-particle configurations carrying total intrinsic spin of the protons and neutrons equal to zero and one, with the largest contribution due to $(S_p\, S_n\, S) = (0\,0\,0)$ configurations. This is illustrated in Figure 1b for the ground state of ^{8}Be.

The mixing of $(\lambda\,\mu)$ spatial quantum numbers induced by the SU(3) symmetry breaking terms of realistic interactions, exhibits a remarkably simple coherent pattern. One of its key features is the preponderance of a single $0\hbar\Omega$ SU(3) irrep, the so-called leading irrep, that is, the one characterized by the largest value of the second order SU(3) Casimir invariant, $\hat{C}_2$, and hence corresponding to a large intrinsic

Table 1: Probability amplitude of the dominant $(S_p\, S_n\, S)$ spin configuration and the dominant nuclear shapes according to Eq. (2) for the ground state of p-shell nuclei.

Nucleus	$(S_p\, S_n\, S)$	Prob. [%]	$(\lambda_0\, \mu_0)$	Prob. [%]
^{6}Li	$(\frac{1}{2}\, \frac{1}{2}\, 1)$	93.26	$(2\, 0)$	98.13
^{8}B	$(\frac{1}{2}\, \frac{1}{2}\, 1)$	85.17	$(2\, 1)$	87.94
^{8}Be	$(0\, 0\, 0)$	85.25	$(4\, 0)$	90.03
^{12}C	$(0\, 0\, 0)$	55.19	$(0\, 4)$	48.44
^{16}O	$(0\, 0\, 0)$	83.60	$(0\, 0)$	89.51

quadrupole deformation [18]. For instance, the low-lying $T = 0$ states of ^{6}Li project at 40%-70% level onto the prolate-like $0\hbar\Omega$ SU(3) irrep $(2\, 0)$. For the considered states of ^{8}B, ^{8}Be, ^{12}C, and ^{16}O, qualitatively similar dominance of the leading $0\hbar\Omega$ SU(3) irreps is observed – $(2\ 1)$, $(4\ 0)$, $(0\ 4)$, and $(0\ 0)$ irreps, associated with triaxial, prolate, oblate, and spherical shapes, respectively. Such a clear dominance of the largest $0\hbar\Omega$ deformation within the low-lying states of p-shell nuclei points to the fact that the effective quadrupole-quadrupole interaction of the Elliott SU(3) model of nuclear rotations [11] is realized naturally within the framework of modern realistic interactions.

The analysis reveals that the dominant SU(3)-scheme states at each $N\hbar\Omega$ subspace are typically those with $(\lambda\, \mu)$ quantum numbers such that

$$\lambda + 2\mu = \lambda_0 + 2\mu_0 + N, \qquad N = 0, 2, \ldots, \tag{2}$$

where λ_0 and μ_0 denote labels of a leading SU(3) irrep at the $0\hbar\Omega$ ($N = 0$) subspace (Table 1). We conjecture that this coherent pattern of SU(3) quantum numbers reflects the presence of an underlying symplectic $\mathrm{Sp}(3,\mathbb{R})$ symmetry of microscopic nuclear collective motion [12] that governs the low-energy structure of both even-even and odd-odd p-shell nuclei. This can be seen from the fact that configurations with a $(\lambda\, \mu)$ shape that satisfies condition (2) can be determined from the leading SU(3) irrep $(\lambda_0\, \mu_0)$ through a successive application of a specific subset of the $\mathrm{Sp}(3,\mathbb{R})$ symplectic $2\hbar\Omega$ raising operators. This subset is composed of the three operators, $\hat{A}_{zz}, \hat{A}_{zx}$, and $\hat{A}_{xx}$, that distribute two oscillator quanta in z and x directions, but none in y direction, thereby inducing SU(3)-scheme configurations with ever-increasing values of the Casimir invariant $\hat{C}_2$. These three operators are the generators of the $\mathrm{Sp}(2,\mathbb{R}) \subset \mathrm{Sp}(3,\mathbb{R})$ subgroup [19], and give rise to a hierarchy of deformed shapes that are energetically favored by an attractive quadrupole-quadrupole interaction [13]. Furthermore, there is an apparent hierarchy among states that fulfill condition (2). In particular, the $N\hbar\Omega$ configurations with $(\lambda_0{+}N\ \mu_0)$, the so-called stretched states, carry a noticeably higher intensity than the others. For instance, the $(2+N\ 0)$ stretched states contribute at the 85% level to the ground state of ^{6}Li. The sequence of the stretched-states, that is, the states with the highest possible deformations, can be formed from many-nucleon correlations of a leading SU(3) irrep by application of the $\hat{A}_{zz}$ operator, which is the generator of $\mathrm{Sp}(1,\mathbb{R}) \subset \mathrm{Sp}(2,\mathbb{R}) \subset \mathrm{Sp}(3,\mathbb{R})$ subgroup.

The revealed pattern of intrinsic spin and deformation mixing supports a symmetry guided truncation of the $N_{\max}$ model space. Clearly, one can take advantage of the physical relevance of the SU(3)-scheme basis to winnow the full space down to the most relevant configurations that support the strongest many-nucleon correlations of the system using the underlying $\mathrm{Sp}(1,\mathbb{R}) \subset \mathrm{Sp}(2,\mathbb{R}) \subset \mathrm{Sp}(3,\mathbb{R})$ symmetry considerations. As noted previously, this truncation, while significantly reducing the size of the model space, also preserves the ability to factor out exactly the spurious center-of-mass degrees of freedom.

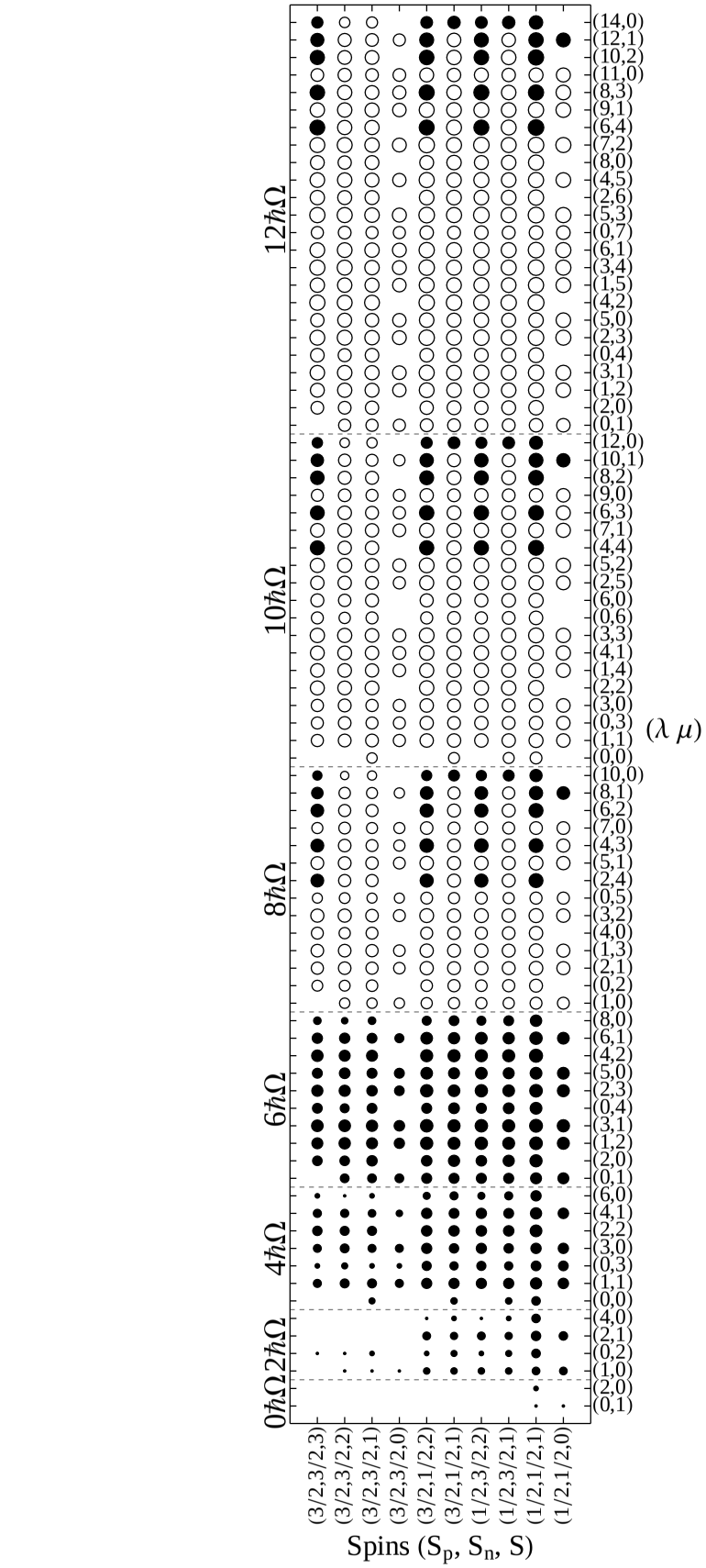

Figure 2: Pauli-allowed $(\lambda\,\mu)$ deformations and their proton, neutron, and total intrinsic spins $(S_p\,S_n\,S)$ for the positive-parity $J = 1$ states of ^{6}Li spanning the full $N_{\max} = 12$ model space. Each circle represents basis states carrying the same $N\,(\lambda\,\mu)\,S_pS_nS$ quantum numbers, with the radius being proportional to $\log_{10}$ of the number of such states. Configurations symbolized by the filled circles constitute the symmetry-truncated model space 12[6].

4 Efficacy of the SU(3) basis

To probe the adequacy of the symmetry-adapted approach for the *ab initio* modelling of nuclear structure, we used the calculated eigenstates to determine spectroscopic properties of low-lying $T = 0$ states of ^{6}Li using a model space winnowed through symmetry considerations, and compared the outcomes with the corresponding results obtained in the full $N_{\max} = 12$ space. In the study, Coulomb and bare JISP16 NN interactions were used for $\hbar\Omega$ oscillator strengths ranging from 17.5 up to 25 MeV. The selected model space, depicted in Fig. 2 and denoted by 12[6], incorporates all configurations carrying excitations up to 6 oscillator quanta (labeled by [6]) and only a subset of the shapes and a few intrinsic spin components to realize the leading modes of nuclear collective motion for the higher $8\hbar\Omega, 10\hbar\Omega$ and $12\hbar\Omega$ configurations. The model space 12[6] constitutes a small percentage of the full space. For example, the full $N_{\max} = 12$ model space dimension is 4.9×10^7 whereas the dimensions of the 12[6] subspaces with total angular momenta $J = 1$, $J = 2$, and $J = 3$, are 4.3×10^5 (0.87%), 6.5×10^5 (1.32%), and 8.3×10^5 (1.70%), respectively.

The ground state binding energies calculated in 12[6] for oscillator energy $\hbar\Omega$ ranging from 17.5 to 25 MeV represent from 98% up to 98.7% of the full-space binding energy. Furthermore, the excitation energies of 3^+_1, 2^+_1, and 1^+_2 states calculated in 12[6] model space differ only by 20 keV to a few hundreds of keV from the corresponding full-space results, see Fig. 3.

As illustrated in Table 2 for $\hbar\Omega = 17.5$ MeV, the magnetic dipole moments agree to within less than about 0.3%, or 5% for the $\mu(2^+_1 0)$. As the dipole moment is a short-range operator, the results suggest that it may suffice to include all low-lying $\hbar\Omega$ states up to a fixed limit, e. g. $N_{\max} = 6$ for ^{6}Li, to account for the most important short-range correlations.

To explore how closely one comes to reproducing the important long-range correlations of the full $N_{\max} = 12$ space in terms of nuclear collective excitations within the more restricted 12[6] space, we compared observables that are sensitive to the tails of the wave functions; specifically, the point-particle rms matter radii, the electric quadrupole moments and the reduced electromagnetic $B(E2)$ transition strengths. The results for the rms matter radii, listed in Table 2 for $\hbar\Omega = 17.5$ MeV, agree to within 1%. Similarly, the 12[6] eigensolutions yield results for these quantities that track very closely with their full [12] space counterparts for all values of $\hbar\Omega$, as can be

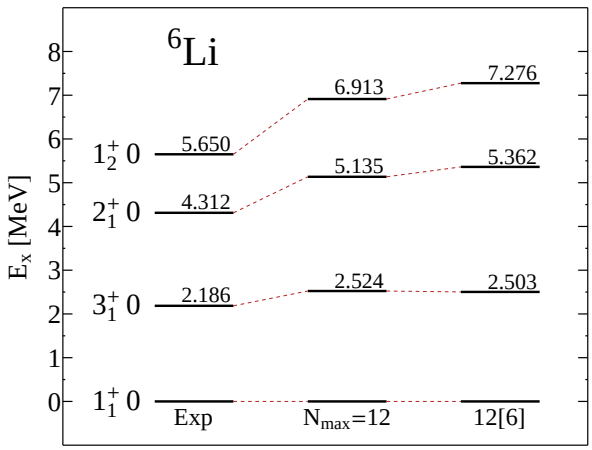

Figure 3: Experimental and theoretical excitation energies of $T = 0$ states of ^{6}Li. Theoretical estimates were obtained at $\hbar\Omega = 22.5$ MeV in the full $N_{\max} = 12$ (middle) and the symmetry-truncated 12[6] (right) model spaces.

Table 2: Magnetic dipole moments μ [μ_N] and point-particle rms matter radii [fm] of $T = 0$ states of ^{6}Li calculated in the full $N_{\max} = 12$ and 12[6] model spaces for $\hbar\Omega = 17.5$ MeV. The experimental value for the 1^+ ground state is known to be $\mu = +0.822\ \mu_N$.

	$1^+_1 0$	$3^+_1 0$	$2^+_1 0$	$1^+_2 0$
	μ			
Full $N_{\max} = 12$	0.838	1.866	0.960	0.336
12[6] SU(3)	0.840	1.866	1.015	0.337
	rms			
Full $N_{\max} = 12$	2.146	2.092	2.257	2.373
12[6] SU(3)	2.139	2.079	2.236	2.355

seen in Fig. 4. Also, as the $B(E2)$ strengths almost doubles upon increasing the basis space from $N_{\max} = 6$ to $N_{\max} = 12$ — a result that suggests that further expansion of the basis space may be needed to reach the experimental value of 21.8(4.8) e^2fm^4, the close correlation between the $N_{\max} = 12$ and 12[6] results is even more impressive.

5 Conclusion

We have developed a novel approach that capitalizes on advances being made in *ab initio* methods while exploiting exact and partial symmetries of nuclear many-body system. Using this approach we have demonstrated that the low-lying eigenstates of ^{6}Li, ^{8}Be, ^{12}C, and ^{16}O, which were obtained using the JISP16 NN interaction, exhibit a strong dominance of few intrinsic spin components and carry an intriguingly simple pattern of dominant deformations. The results very clearly underscore the significance of the SU(3) scheme, LS-coupling, and underlying symplectic symmetry in enabling an extension, through symmetry-guided model space reductions, of *ab initio* methods to heavier nuclei beyond ^{16}O.

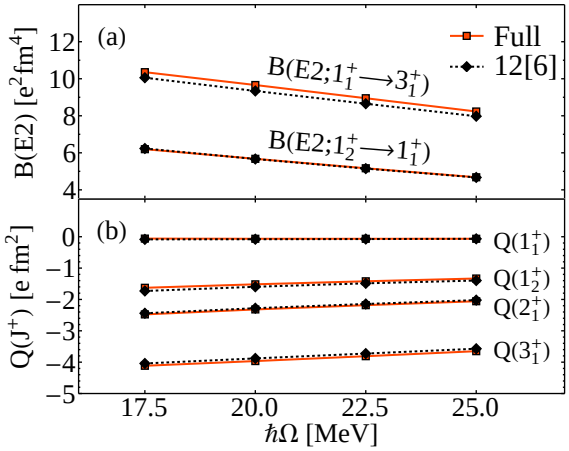

Figure 4: Electric quadrupole transition probabilities (a) and quadrupole moments (b) as a function of $\hbar\Omega$ for T=0 states of ^{6}Li calculated in the full $N_{\max} = 12$ (solid red line) and symmetry-truncated 12[6] (dashed black line) model spaces.

Acknowledgments

This work was supported by the National Science Foundation under Grants No. PHY-0500291 and OCI-0904874, the US Department of Energy under Grants No. DEFG02-95ER-40934 and DE-SC0005248, the Southeastern Universities Research Association, and by the Research Corporation for Science Advancement under a Cottrell Scholar Award. This research used computing resources of the Louisiana Optical Network Initiative, LSU's Center for Computation & Technology, and the National Energy Research Scientific Computing Center, which is supported by the Office of Science of the U.S. Department of Energy under Contract No. DE-AC02-05CH11231.

References

[1] A. M. Shirokov, J. P. Vary, A. I. Mazur and T. A. Weber, Phys. Lett. B **644**, 33 (2007).

[2] R. B. Wiringa, V. G. J. Stoks and R. Schiavilla, Phys. Rev. C **51**, 38 (1995).

[3] D. R. Entem and R. Machleidt, Phys. Rev. C **68**, 041001 (2003).

[4] E. Epelbaum, Prog. Part. Nucl. Phys **57**, 654 (2006).

[5] P. Navrátil, J. P. Vary and B. R. Barrett, Phys. Lett. **84**, 5728 (2000).

[6] S. C. Pieper, K. Varga and R. B. Wiringa, Phys. Rev. C **66**, 044310 (2002).

[7] M. Wloch, D. J. Dean, J. R. Gour, M. Hjorth-Jensen, K. Kowalski, T. Papenbrock and P. Piecuch, Phys. Rev. Lett. **94**, 212501 (2005).

[8] P. Navrátil, S. Quaglioni, I. Stetcu and B. R. Barrett, J. Phys. G **36**, 083101 (2009).

[9] R. Roth and P. Navrátil, Phys. Rev. Lett. **99**, 092501 (2007).

[10] P. Navratil, V. G. Gueorguiev, J. P. Vary, W. E. Ormand and A. Nogga, Phys. Rev. Lett. **99**, 042501 (2007); arXiv: nucl-th/0701038 (2007).

[11] J. P. Elliott, Proc. Roy. Soc. A **245**, 128 (1958).

[12] G. Rosensteel and D. J. Rowe, Phys. Rev. Lett. **38**, 10 (1977).

[13] D. J. Rowe, Rep. Prog. Phys. **48**, 1419 (1985).

[14] F. Q. Luo, M. A. Caprio and T. Dytrych, Nucl. Phys. A, *in press* (2012), http://dx.doi.org/10.1016/j.nuclphysa.2012.11.003; arXiv:1211.3187 [nucl-th] (2012).

[15] J. P. Draayer, Y. Leschber, S. C. Park and R. Lopez, Comput. Phys. Comm. **56**, 279 (1989).

[16] C. Bahri and J. P. Draayer, Comput. Phys. Comm. **83**, 59 (1994).

[17] Y. Akiyama and J. P. Draayer, Comput. Phys. Comm. **5**, 405 (1973).

[18] O. Castanos, J. P. Draayer and Y. Leschber, Z. Phys. A **329**, 33 (1988).

[19] D. R. Peteron and K. T. Hecht, Nucl. Phys. A **344**, 361 (1980).